ISSN 1070-3284, Russian Journal of Coordination Chemistry, 2008, Vol. 34, No. 8, pp. 584–593. © Pleiades Publishing, Ltd., 2008.
Original Russian Text © A.V. Ivanov, I.A. Lutsenko, M.A. Ivanov, A.V. Gerasimenko, O.N. Antzutkin, 2008, published in Koordinatsionnaya Khimiya, 2008, Vol. 34, No. 8, pp. 591–600.

Synthesis, Structural and Multinuclear Natural Abundance (^{13}C, ^{31}P, ^{195}Pt) CP/MAS NMR Studies of Crystalline O,O'-Dialkyldithiophosphate Platinum(II) Complexes

A. V. Ivanov[a], I. A. Lutsenko[a], M. A. Ivanov[a], A. V. Gerasimenko[b], and O. N. Antzutkin[c]

[a]*Institute of Geology and Nature Management, Amur Scientific Center, Far East Division, Russian Academy of Sciences, Blagoveshchensk, 675000 Russia*

[b]*Institute of Chemistry, Far East Division, Russian Academy of Sciences, pr. Stoletiya Vladivostoka 159, Vladivostok, 690022 Russia*

[c] *Luleå University of Technology, S-97187, Luleå, Sweden*

E-mail: alexander.v.ivanov@chemist.com

Received June 26, 2007

Abstract—Platinum(II) O,O'-dicyclohexyl dithiophosphate [Pt{S_2P(O-*cyclo*-C_6H_{11})$_2$}$_2$] (**I**) and platinum(II) O,O'-diisopropyl dithiophosphate [Pt{S_2P(O-*iso*-C_3H_7)$_2$}$_2$] (**II**) complexes were obtained and studied by solid-state ^{13}C, ^{31}P, and ^{195}Pt CP/MAS NMR spectroscopy. The dithiophosphate (Dtph) ligands in molecular structure **I** were found to be coordinated by platinum in S,S'-bidentate fashion to form the planar chromophore [PtS_4] (single-crystal X-ray diffraction data). For complex **II**, a new α-form (α-**II**) was obtained and identified by ^{31}P MAS NMR spectroscopy. The ^{31}P chemical shift anisotropy δ_{aniso} and the asymmetry parameter η of the ^{31}P chemical shift tensor were calculated from the whole MAS spectra.

DOI: 10.1134/S1070328408080058

Most of the hitherto known platinum(II) O,O'-dialkyldithiophosphates are liquids or oily compounds [1]. Only two crystalline platinum complexes [Pt{$S_2P(OR)_2$}$_2$] have been structurally characterized: R = C_2H_5 [1] and *iso*-C_3H_7 [2]. In [3], we have demonstrated with single-crystal cooperite (natural PtS) as an example that ^{195}Pt (both static and MAS) NMR spectroscopy can be employed for investigation of natural minerals of platinum. In cooperite, platinum(II) is included in square chromophores [PtS_4]. However, a structurally similar pattern has been found in dialkyl dithiophosphates [1, 2]: the metal atom is surrounded by four sulfur atoms making a slightly distorted square. That is why we found it interesting to obtain crystalline platinum(II) dialkyl dithiophosphates and compare their ^{195}Pt MAS NMR spectra and X-ray diffraction patterns.

In this study, we obtained the new complexes bis(O,O'-dicyclohexyldithiophosphato-S,S')platinum(II) (**I**) and bis(O,O'-diisopropyldithiophosphato-S,S')platinum(II) (**II**) of the general formula [Pt{$S_2P(OR)_2$}$_2$] (R = *cyclo*-C_6H_{11} (**I**) and the α-form for R = *iso*-C_3H_7 (**II**)) and the magnetically diluted (with Pt(II)) isotope-substituted complex bis(O,O'-dicyclohexyldithiophosphato-S,S')copper(II) [^{63}Cu{S_2P(O-*cyclo*-C_6H_{11})$_2$}$_2$] (**III**). The structures of these complexes were studied by ^{13}C, ^{31}P, and ^{195}Pt CP/MAS NMR spectroscopy and EPR spectroscopy; structure **I** was characterized by X-ray diffraction data.

EXPERIMENTAL

Synthesis. Crystalline complexes **I** and **II** were obtained by reactions of aqueous solutions of $K_2[PtCl_4]$ and appropriate salts K{$S_2P(OR)_2$}. The reaction mixtures were heated at 60°C for a short period of time and left overnight. The resulting yellow precipitates were filtered off, washed with water, and dried on the filter. Additional crops were obtained by extraction of the complexes from the mother liquors by chloroform. Single crystals of complex **I** for X-ray diffraction analysis were obtained from chloroform.

For EPR study, complex **III** was synthesized in the magnetically diluted state by mechanically grinding complex **I** with a small amount of $CuCl_2 \cdot 2H_2O$ (Cu : Pt = 1 : 1000). The use of this technique allows the molecules of complex **III** to be stabilized in the matrix of the platinum(II) complex.[1] The content of the ^{63}Cu isotope in $CuCl_2 \cdot 2H_2O$ was 99.3(1) at %.

[1] Copper(II) O,O'-dialkyl dithiophosphates do not exist in the individual state because of prompt conversion into polynuclear copper(I) complexes [4] and the corresponding bis(O,O'-dialkylthiophosphoryl) disulfides according to the intermolecular redox reaction:

$$4Cu^{2+} + 8(RO)_2P(S)S^- = 4[Cu\{S_2P(OR)_2\}_2]$$
$$= [Cu_4\{S_2P(OR)_2\}_4] + 2(RO)_2P(S)S–S(S)P(OR)_2.$$

Crystalline complexes **I** and **II** and the starting potassium dithiophosphates were characterized by ^{13}C MAS NMR spectroscopy:

Complex **I**, δ: (1 : 2 : 1 : 2) 76.2, 76.1 (1 : 1, –OCH=), 32.9, 32.2 (1 : 1, *o*-CH_2–), 26.2, 26.0 (*p*-CH_2–), 21.4, 20.8 ppm (*m*-CH_2–).

K{S_2P(O-*cyclo*-$C_6H_{11})_2$}, δ: (1 : 2 : 3) 79.9, 78.8, 78.1, 77.1 (1 : 1 : 1 : 1, –OCH=), 35.7, 35.2, 34.7, 33.9 (*o*-CH_2–), 26.2 ppm (*m*-, *p*-CH_2–).

α-**II**, δ: (1 : 2) 74.1 (–OCH=), 26.5, 26.2, 25.7, 25.0 ppm (1 : 1 : 1 : 1, –CH_3).

[Pt{S_2P(O-*iso*-$C_3H_7)_2$}$_2$] (β-**II**), δ: (1 : 2) 73.1 (–OCH=), 25.2, 24.9, 24.6, 24.0 ppm (2 : 3 : 2 : 1, –CH_3).

K{S_2P(O-*iso*-$C_3H_7)_2$}, δ: (1 : 2) 73.0, 72.8, 70.5, 69.9 (1 : 1 : 1 : 1, –OCH=), 27.0, 26.7, 26.3, 25.4, 25.0, 24.1 ppm (1 : 1 : 2 : 6 : 2 : 4, –CH_3).

EPR spectra were recorded on a 70-02 XD/1 radio spectrometer (~9.5 GHz) at ~295 K. The operating frequency was measured with a ChZ-46 microwave frequency meter. *g* Factors were calculated with reference to DPPH. The error in the determination of *g* factors was ±0.002; the constants of the hyperfine (HFS) and extra hyperfine structures (EHFS) are quoted in oersteds (Oe) to within ±2%. EPR spectra were modeled to the second order of perturbation theory with the WIN-EPR SimFonia program (Bruker software, version 1.2). *g* Factors, HFS and EHFS constants, resonance line widths, and percent contributions from the Lorentzian and Gaussian functions to the line shapes were variables of the modeling.

^{13}C, ^{31}P, and ^{195}Pt MAS NMR spectra were recorded on a CMX-360 spectrometer operating at 90.52, 145.72, and 76.99–77.22 MHz, respectively (superconducting magnet with B_0 = 8.46 T; Fourier transform). The ^{13}C–^1H and ^{31}P–^1H cross polarization techniques were used; ^{13}C–^1H and ^{31}P–^1H dipolar interactions were suppressed via proton decoupling in a magnetic field with the corresponding proton resonance frequency [5]. Samples (~300 mg) of the complexes were packed into a zirconia rotor (7.5 mm in diameter). The spinning frequencies in $^{13}C/^{31}P$ MAS NMR experiments were 4000–5500/3200–5000(1) Hz. The numbers of scans were 1200–5200/256–400, respectively. The proton π/2 pulse durations were 5.4/5.4 μs. The ^1H–$^{13}C/^1H$–^{31}P contact times were 1.5/2.0 ms; the pulses were spaced at 3.0/3.0 s. Isotropic ^{13}C, ^{31}P, and ^{195}Pt chemical shifts **δ** (ppm) are referenced to a line of crystalline adamantane [6] used as the external standard (δ 38.48 ppm relative to tetramethylsilane [7]), 85% H_3PO_4(0 ppm) [8], and aqueous 0.1 M $H_2[PtCl_6]$ (0 ppm; the corresponding ^{195}Pt resonance frequency is (77.3768 MHz) [9], respectively.

In ^{195}Pt MAS NMR experiments, we used a 60° direct excitation pulse with a 3.7-μs duration to excite a spectral range of 45 kHz. ^{195}Pt–^1H interactions were suppressed via proton decoupling in a magnetic field (amplitude $\gamma B_1/2\pi$ = 46.9 kHz) with the corresponding proton resonance frequency (359.945 MHz). The total width of experimental ^{195}Pt MAS NMR spectra (~290 kHz) made it impossible to simultaneously excite the entire spectrum at a single carrier frequency. For this reason, we varied the carrier frequency with a step of 77 kHz to excite different regions of the spectrum. The whole pattern was obtained by summation of the individual spectra recorded at 76.991, 77.068, 77.145, and 77.222 MHz. The summation was preceded by shifting the spectra so that the central signal and all sidebands coincided exactly. The spinning frequency was 5000(1) Hz. For each fragment, the number of scans was 20 000 (for **I**) and 16 800 (for β-II); the pulses were spaced at 3.0 s. Since the initial region of the free induction decay (FID) diagrams of the MAS NMR spectra was distorted by the decay of the exciting pulse (due to the "ringdown" effect), the distorted range was cut off. To avoid phase distortions of the MAS NMR spectrum, the FID diagram was shifted before Fourier transforms to the decay region by a required number of points. Since the FID diagrams contained over 15 (**I**) or 27 rotational echoes (β-II), removal of the initial fragment did not result in critical spectral changes. The magic angle was set by observing the ^{79}Br resonance frequency of crystalline KBr (90.189 MHz) according to a standard procedure. Its adjustment was performed by minimizing the line widths in the ^{195}Pt MAS NMR spectrum of natural single-crystal cooperite (PtS), which is characterized by a considerable ^{195}Pt chemical shift anisotropy (δ_{aniso} = 5873 ppm, η = 0.37 [3]) and, consequently, by a high sensitivity of the line width to small deviations of the magic angle.

The width of the reference line for crystalline adamantane (3.5 Hz) was used to check the homogeneity of the magnetic field. The δ_{iso} values were corrected for drift of the magnetic field strength during the measurements (its frequency equivalents for the $^{13}C/^{31}P/^{195}Pt$ nuclei were 0.051/0.11/0.044 Hz/h). The chemical shifts, the integrated intensity ratios for the overlapping signals, and the coupling constants were refined by fragment-by-fragment mathematical modeling of NMR spectra with regard to the line positions and widths and the contributions from the Lorentzian and Gaussian functions to the line shapes. The ^{31}P chemical shift anisotropy ($\delta_{aniso} = (\delta_{zz} - \delta_{iso})$ and the asymmetry parameter of the ^{31}P chemical shift tensor ($\eta = (\delta_{yy} - \delta_{xx})/(\delta_{zz} - \delta_{iso})$) were calculated from diagrams of the χ^2 statistics [10]. Plotting of the diagrams was based on quantitative analysis of the integrated intensity ratios for sidebands (due to spinning) [11, 12] in the spectra recorded at two different spinning frequencies. The calculations were performed with the Mathematica program (version 4.1.2) [13].

Single-crystal X-ray diffraction analysis of complex **I** was performed on a BRUKER SMART 1000 CCD diffractometer (MoK_α radiation, λ = 0.71073 Å, graphite monochromator) at 173(1) K. Reflections were collected in the hemisphere [14] (crystal–detector

Table 1. Crystallographic parameters and a summary of data collection and refinement for structure I

Parameter	Value
Empirical formula	$C_{24}H_{44}O_4P_2S_4Pt$
M	781.86
Crystal system	Monoclinic
Space group	$P2_1/n$
a, Å	11.854(2)
b, Å	9.354(1)
c, Å	13.879(2)
β, deg	96.49(1)
V, Å^3	1529.0(4)
Z	2
ρ(calcd.), g/cm^3	1.698
μ, mm^{-1}	4.994
F(000)	784
Crystal shape (size, mm)	Prism (0.38 × 0.29 × 0.15)
θ scan range, deg	2.14–35.50
Ranges of h, k, and l indice	$-19 \le h \le 19$ $-10 \le k \le 15$ $-20 \le l \le 22$
Number of measured reflections	18152
Number of independent reflections	6882 (R_{int} = 0.0317)
Number of reflections with $I > 2\sigma(I)$	5306
Number of parameters refined	160
GOOF	1.036
R factors for $F^2 > 2\sigma(F^2)$	R_1 = 0.0291 wR_2 = 0.0697
R factors for all reflections	R_1 = 0.0426 wR_2 = 0.0760
Residual electron density (min/max), e Å^{-3}	–1.031/1.651

Table 2. Atomic coordinates and isotropic equivalent thermal parameters U_{equiv} for structure I

Atom	x	y	z	U_{equiv}, Å^2
Pt	0.5	0	1.0	0.02425(1)
S(1)	0.54270(2)	0.20845(3)	0.91931(2)	0.04086(7)
S(2)	0.69145(2)	0.00550(3)	1.05985(2)	0.03769(7)
P	0.70569(2)	0.17069(3)	0.96893(2)	0.03132(6)
O(1)	0.78497(7)	0.14300(8)	0.88807(6)	0.0415(2)
O(2)	0.77179(6)	0.30320(8)	1.01485(5)	0.0387(2)
C(1)	0.7802(1)	0.0119(1)	0.82892(9)	0.0379(3)
C(2)	0.7795(1)	0.0585(2)	0.7266(1)	0.0559(4)
C(3)	0.8928(2)	0.1375(2)	0.7123(1)	0.0830(6)
C(4)	0.9964(1)	0.0471(2)	0.7573(2)	0.0852(5)
C(5)	0.9885(1)	0.0014(2)	0.8576(2)	0.0626(5)
C(6)	0.8818(1)	–0.0741(1)	0.8637(1)	0.0625(5)
C(7)	0.73484(9)	0.3769(1)	1.09980(7)	0.0358(2)
C(8)	0.7156(1)	0.5316(2)	1.0712(1)	0.0599(4)
C(9)	0.8258(2)	0.6033(2)	1.0514(1)	0.0670(5)
C(10)	0.9182(2)	0.5863(2)	1.1347(1)	0.0773(5)
C(11)	0.9368(1)	0.4315(2)	1.1602(1)	0.0622(5)
C(12)	0.8277(1)	0.3600(2)	1.18200(8)	0.0461(3)

distance 38 mm, ω scan mode, scan step 0.2°, frame exposure time 20 s). Absorption correction was applied from the face indices of the single crystal. Structure **I** was solved by the direct method and refined by the least-squares method (on F^2) in the full-matrix anisotropic approximation for non-hydrogen atoms. The hydrogen atoms were located geometrically and refined in the rider model. The collected data were edited and the unit cell parameters were refined with the SMART and SAINT-*Plus* programs [14]. All calculations for structure determination and refinement were performed with the SHELXTL/PC programs [15].

Selected crystallographic parameters and a summary of data collection and refinement for structure **I** are summarized in Table 1. Atomic coordinates and thermal parameters are listed in Table 2. Bond lengths and angles are given in Table 3.

RESULTS AND DISCUSSION

The EPR spectrum of isotope-substituted complex **III** magnetically diluted with platinum(II) is close to the axially symmetric pattern (Fig. 1a). The EPR parameters were refined by computer-assisted modeling of spectra (Fig. 1b), which revealed some anisotropy of the *g*- and *A* tensors in the plane *xy*:

$g_\parallel$	$A_\parallel^{Cu}$, Oe	$A_\parallel^{P}$, Oe	$g_\perp$	$A_\perp^{Cu}$, Oe	$A_\perp^{P}$, Oe
2.088	154	9.6	2.025	36.0	9.7
			2.023	35.8	9.7

Each orientation of the EPR spectrum shows a quartet of the HFS components due to the ^{63}Cu nucleus (I = 3/2) and an intense high-field extra absorption (EA) peak [16, 17]. All the HFS components and the EA peak are additionally split into triplets (1 : 2 : 1) of the EHFS components due to the ^{31}P nuclei (I = 1/2) in two structurally equivalent Dtph ligands. The aforesaid *g* factors and HFS constants suggest the presence of the square chromophores [CuS_4] in structure **III**. The anisotropy of the EPR parameters in the plane *xy* we noted above can arise from a rhombic distortion of the chromophore because of some nonequivalence of *cis*-oriented Cu–S bonds.

The ^{13}C MAS NMR spectra of complexes **I** and **II** (Fig. 2) contain signals for the –OCH=, *o*-CH_2–, *m*-CH_2–, *p*-CH_2–, and –CH_3 groups of the alkyl substituents in the dithiophosphate ligands. Pairs of ^{13}C NMR signals for the *o*-, *m*-, and *p*-carbon atoms in the (*cyclo*-$C_6H_{11}O)_2PS_2^-$ ligands (Fig. 2a) suggest that the cyclic –C_6H_{11} fragments are structurally nonequivalent. Complex **II** exists in two spectrally different forms, depending on the conditions of its synthesis: precipitation from the aqueous phase mainly gives the α-form, while crystallization from chloroform yields the β-form (Figs. 2b, 2c).

Each signal in the ^{31}P MAS NMR spectra of complexes **I** and **II** (Fig. 3) has two symmetrically arranged satellite signals (~1 : 4 : 1). Because naturally occurring platinum contains the ^{195}Pt nuclide (33.83 at %, μ = 0.60950 μN; I = 1/2), the observed multiplet structure of the signals under discussion results from isotropic ^{31}P–^{195}Pt spin-spin couplings with the coupling constant $^2J(^{31}P–^{195}Pt)$ (Table 4). The sole ^{31}P NMR signal in the center of gravity of the spectrum of complex **I** (Fig. 3a) is indicative of the structural equivalence of the Dtph ligands. The spectrum suggests the presence of a small amount of a complex with the larger chemical shift: $\delta(^{31}P)$ = 101.9 ppm and $^2J(^{31}P–^{195}Pt)$ = 431 Hz. A comparison of the ^{31}P MAS NMR spectra of the samples of complex **II** obtained by precipitation from the aqueous phase (Fig. 3b) and crystallization from chloroform (Fig. 3c) showed that the former sample contains both α- and β-forms (~30%). Additional inflec-

Table 3. Selected bond lengths and angles in structure I

Bond	*d*, Å	Bond	*d*, Å
Pt–S(1)	2.3324(4)	C(2)–C(3)	1.564(3)
Pt–S(2)	2.3273(4)	C(3)–C(4)	1.562(3)
S(1)–P	2.0077(5)	C(4)–C(5)	1.469(3)
S(2)–P	2.0141(4)	C(5)–C(6)	1.459(2)
P–O(1)	1.5645(9)	C(7)–C(8)	1.511(2)
P–O(2)	1.5631(8)	C(7)–C(12)	1.501(2)
O(1)–C(1)	1.473(1)	C(8)–C(9)	1.521(2)
O(2)–C(7)	1.474(1)	C(9)–C(10)	1.508(2)
C(1)–C(6)	1.483(2)	C(10)–C(11)	1.501(3)
C(1)–C(2)	1.485(2)	C(11)–C(12)	1.517(2)
Angle	**ω, deg**	**Angle**	**ω, deg**
S(1)PtS(2)	84.10(1)	C(2)C(1)C(6)	112.8(1)
PS(1)Pt	86.61(2)	C(1)C(2)C(3)	110.4(1)
PS(2)Pt	86.60(2)	C(4)C(3)C(2)	110.0(1)
S(1)PS(2)	101.79(2)	C(5)C(4)C(3)	113.9(1)
O(1)PS(1)	114.57(3)	C(6)C(5)C(4)	110.2(2)
O(1)PS(2)	114.97(3)	C(5)C(6)C(1)	113.4(1)
O(2)PS(1)	114.77(3)	O(2)C(7)C(12)	107.47(9)
O(2)PS(2)	115.24(3)	O(2)C(7)C(8)	106.7(1)
O(2)PO(1)	96.30(4)	C(12)C(7)C(8)	112.1(1)
C(1)O(1)P	123.32(7)	C(7)C(8)C(9)	111.3(1)
C(7)O(2)P	121.08(7)	C(10)C(9)C(8)	112.3(1)
O(1)C(1)C(2)	106.52(9)	C(11)C(10)C(9)	110.9(1)
O(1)C(1)C(6)	107.0(1)	C(10)C(11)C(12)	111.5(1)
		C(7)C(12)C(11)	111.8(1)

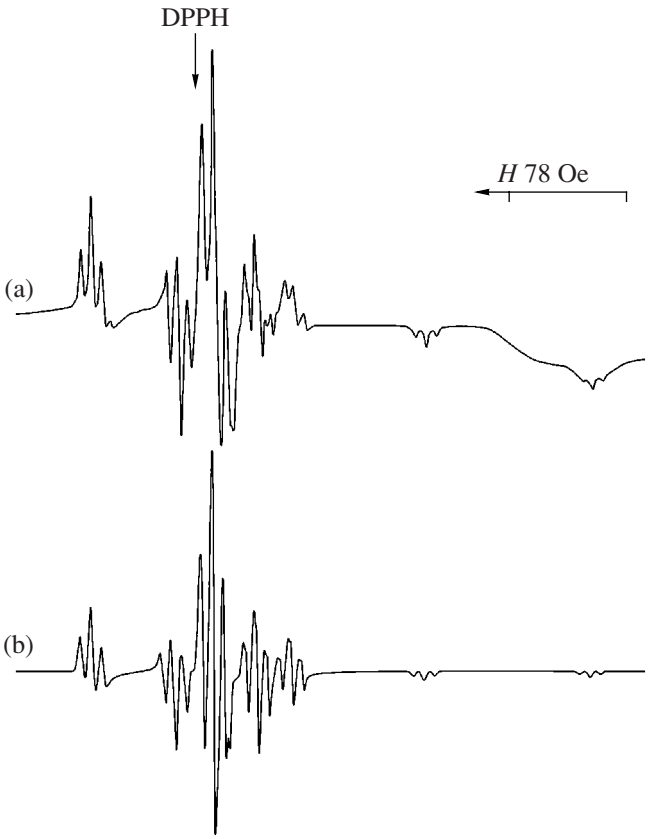

Fig. 1. (a) Experimental and (b) model EPR spectra of the magnetically diluted isotope-substituted complex $[^{63}Cu\{S_2P(O\text{-}cyclo\text{-}C_6H_{11})\}_2]$.

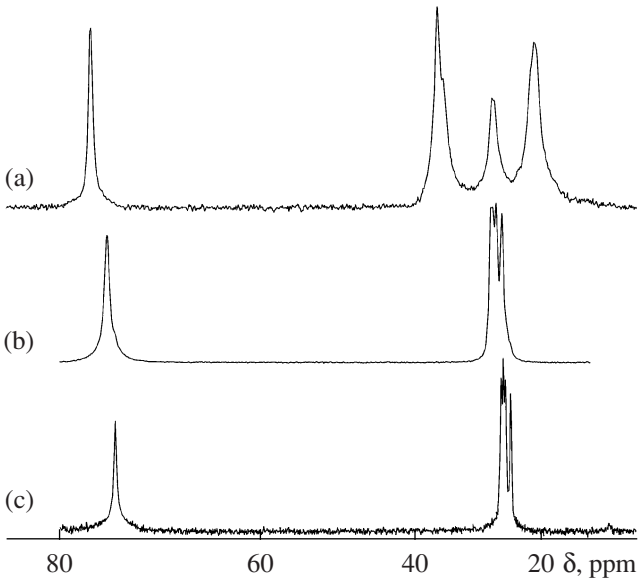

Fig. 2. ^{13}C MAS NMR spectra of the complexes $[Pt\{S_2P(OR)_2\}_2]$: R = (a) *cyclo*-C_6H_{11} and (b, c) *iso*-C_3H_7. The samples were obtained by (a, c) crystallization from chloroform and (b) precipitation from the aqueous phase. The number of scans/spinning frequency (Hz) are (a) 2800/4000, (b) 5200/5500, and (c) 1200/5500.

tions on the triplet components in the ^{31}P NMR spectrum of the α-form of complex **II** can be attributed to the presence of two isomeric molecules in this form.

The shapes of the whole ^{31}P MAS NMR spectra of the complexes obtained suggest a nearly rhombic symmetry of the ^{31}P chemical shift tensors. For quantitative estimation of the ^{31}P chemical shift anisotropy, we plotted diagrams of the χ^2 statistics (Fig. 4) as a function of δ_{aniso} and η. At $\eta = 0$, the chemical shift tensor is axially symmetric. An increase in η from 0 to 1 reflects an

Table 4. Parameters of the ^{31}P and ^{195}Pt MAS NMR spectra of complexes I and II*

Compound	^{31}P				^{195}Pt	
	δ_{iso}, ppm	$^2J_{^{31}P-^{195}Pt}$, Hz	δ_{aniso}, ppm**	η**	δ_{iso}, ppm	$^2J_{^{195}P-^{31}Pt}$, Hz
$[Pt\{S_2P(O\text{-}cyclo\text{-}C_6H_{11})_2\}_2]$ (I)	99.0	433.2 ± 0.5	–30.8 ± 0.2	0.98 ± 0.02	–3963.6	435 ± 15
$K\{S_2P(O\text{-}cyclo\text{-}C_6H_{11})_2\}$ [30]	109.3 105.0 (1 : 1)		–110.6 ± 1.5 –109.1 ± 1.7	0.14 ± 0.10 0.21 ± 0.06		
$[Pt\{S_2P(O\text{-}iso\text{-}C_3H_7)_2\}_2]$ (α-II)	103.4 103.0	422 ± 11 435 ± 15	–35.9 ± 0.4	0.94 ± 0.04		
$[Pt\{S_2P(O\text{-}iso\text{-}C_3H_7)_2\}_2]$ (β-II)	108.5	431.1 ± 0.7	–42.7 ± 0.2	0.75 ± 0.02	–4002.0	427 ± 5
$K\{S_2P(O\text{-}iso\text{-}C_3H_7)_2\}$ [30]	111.7 103.8 (1 : 1)		–104.7 ± 1.3 –116.7 ± 1.1	0.32 ± 0.03 0.07 ± 0.07		

Notes: * The isotropic chemical shifts δ (ppm) are referenced to 85% H_3PO_4 and 0.1 M $H_2[PtCl_6]$.
** $\delta_{aniso} = \delta_{zz} - \delta_{iso}$; $\eta = (\delta_{yy} - \delta_{xx})/(\delta_{zz} - \delta_{iso})$.

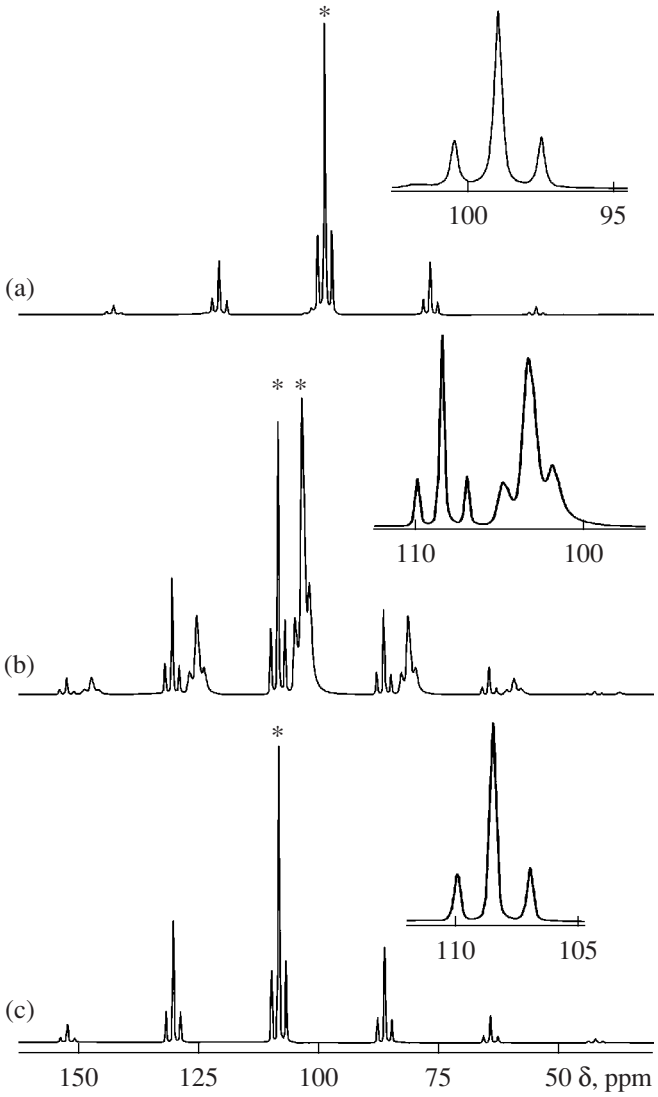

Fig. 3. ^{31}P MAS NMR spectra of the complexes [Pt{$S_2P(OR)_2$}$_2$]: R = (a) *cyclo*-C_6H_{11} and (b, c) *iso*-C_3H_7. The samples were obtained by (a, c) crystallization from chloroform and (b) precipitation from the aqueous phase. The spinning frequency is 3200 Hz; the number of scans is (a) 256, (b) 400, and (c) 64. The signals in the center of gravity of the spectra are asterisked.

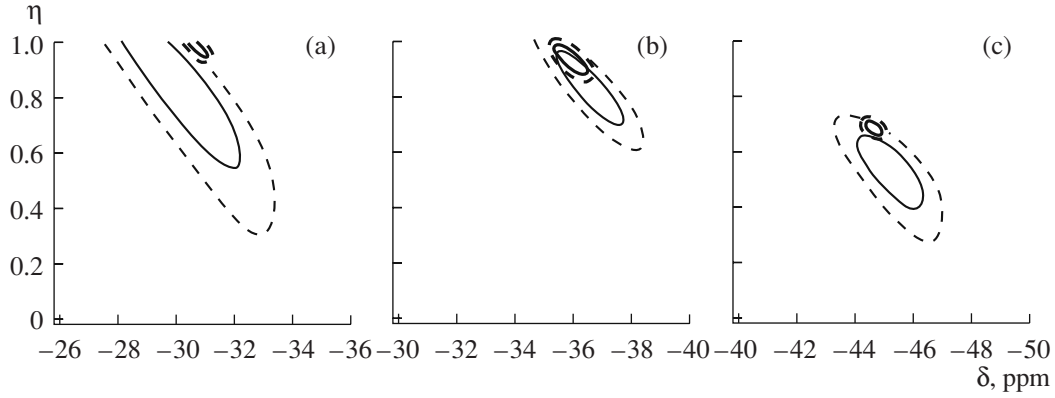

Fig. 4. Diagrams of the χ^2 statistics (as a function of the parameters of the ^{31}P chemical shift anisotropy) of (a) [Pt{$S_2P(O$-*cyclo*-$C_6H_{11})_2$}$_2$] and (b) the α- and β-form and (c) at spinning frequencies of 5000 and 3200 Hz (thin and thick lines, respectively). The solid and dashed lines bound the 68.3% and 95.4% confidence limits, respectively, of δ_{aniso} and η.

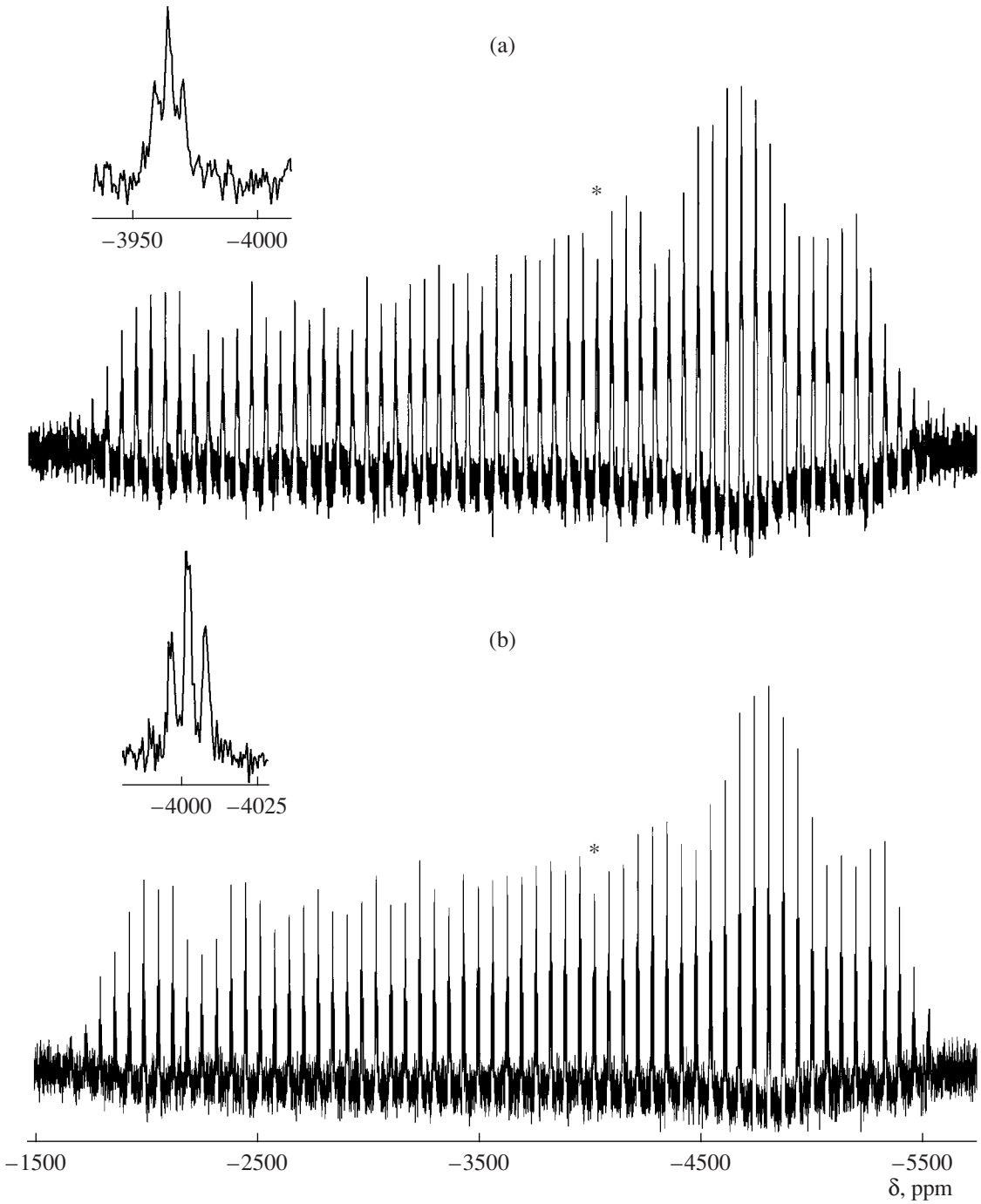

Fig. 5. ^{195}Pt MAS NMR spectra of (a) [Pt{S_2P(O-*cyclo*-C_6H_{11})$_2$}$_2$] and (b) β-[Pt{S_2P(O-*iso*-C_3H_7)$_2$}$_2$]. The samples were obtained by crystallization from chloroform. The spinning frequency is 5000 Hz; the number of scans is (a) 20000 and (b) 16 800. The signals in the center of gravity of the spectra are asterisked.

increasing contribution from the rhombic component. The values η = 0.98–0.75 obtained for the platinum(II) complexes suggest a predominantly rhombic character of the ^{31}P chemical shift tensors. Compared to the nickel(II) [18–20], zinc [19, 21], cadmium [20, 22–24], lead(II) [25–27], silver(I) [28], and antimony(V) dialkyl dithiophosphates [29], complexes **I**, **α-II**, and **β-II** have the lowest δ_{aniso} values (30.8–42.7 ppm). Since δ_{aniso} correlates with the SPS angle [30], we expect that these angles are smallest in the platinum complexes.

The shapes of the whole ^{195}Pt MAS NMR spectra of complexes **I** and β-II (Fig. 5) corresponds to the axially symmetric ^{195}Pt chemical shift tensor (for $\delta_{zz} > \delta_{xx},\delta_{yy}$,

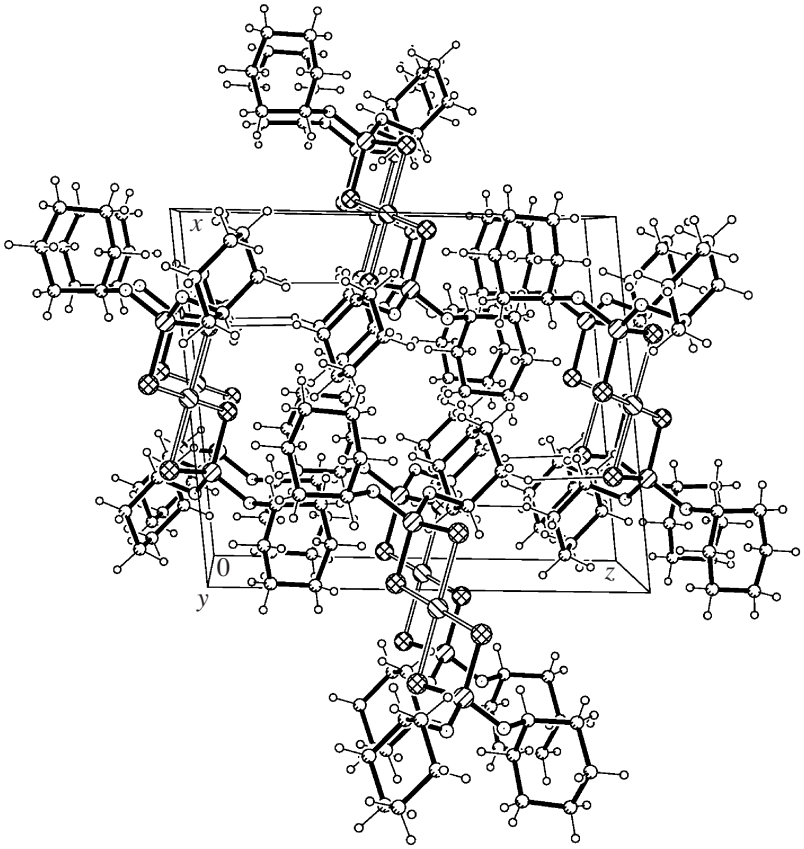

Fig. 6. Projection of the crystal structure of [Pt{S_2P(O-*cyclo*-C_6H_{11})$_2$}$_2$] onto the plane *xz*.

so $\delta_{aniso} > 0$). On the whole, these spectra are similar to the spectrum of single-crystal cooperite (natural PtS) [3] and suggest the formation of square chromophores [PtS_4]. However, the ^{195}Pt chemical shift anisotropy for the platinum(II) complexes is much smaller for the δ_{zz} component, which can be estimated from experimental MAS spectra at –1800 ppm (for PtS, δ_{zz} = +4023 ppm [3]). This also leads to a substantially difference between the isotropic ^{195}Pt chemical shifts. The signals in the center of gravity of the NMR spectra that are characterized by isotropic ^{195}Pt chemical shifts are split into triplets (1 : 2 : 1) due to ^{195}Pt –^{31}P spin-spin couplings on two structurally equivalent Dtph ligands. The coupling constants $^2J(^{195}Pt–^{31}P)$ are given in Table 4.

To verify our conclusions drawn from MAS NMR and EPR spectra, we examined structure **I** by X-ray diffraction analysis.

The unit cell of complex **I** (Fig. 6) consists of two structurally equivalent centrosymmetric molecules [Pt{S_2P(O-*cyclo*-C_6H_{11})$_2$}$_2$] (Fig. 7; Table 3). The platinum atom coordinates two Dtph ligands in S,S'-bidentate fashion to form the planar chromophore [PtS_4] (*dsp*^{2} hybridization state of platinum). The $S_1\cdots S_2$ distance within the ligand (3.121 Å) is noticeably shorter than that between the ligands $S_1\cdots S_2^a$ (3.460 Å)[2]. The slight rhombic distortion of the chromophore is due to the pair nonequivalence of the Pt–S bonds (2.3324 and 2.3273 Å) and the corresponding deviation of the S…S…S angles from 90°. The bidentate coordination of the Dtph ligands produces four-membered chelate rings [PtS_2P]. The torsion PtSSP and SPtPS angles (169.5° and 170.2°, respectively) do not equal 180° because of a tetrahedral distortion of the planar geometry of these rings. In addition, the *trans*-annular Pt…P distances in the chelate rings are very short (2.986 Å).

As expected from ^{31}P MAS NMR data, the S_1PS_2 angle is smallest (101.79°) among all the dithiophosphate complexes we studied earlier [18–30]. The P–S bond lengths (2.0077 and 2.0141 Å) are intermediate between the ideal single (2.14 Å) and double phosphorus–sulfur bonds (1.94 Å) [31]. This is direct evidence for the delocalization of the π-electron density over the structural fragments PS_2. The phosphorus atoms are in a nearly tetrahedral environment [O_2S_2]. The six-membered C_6H_{11} rings are in the chair conformation.

[2] The symmetry operation code is [a] –*x* + 1, –*y*, –*z* + 2.

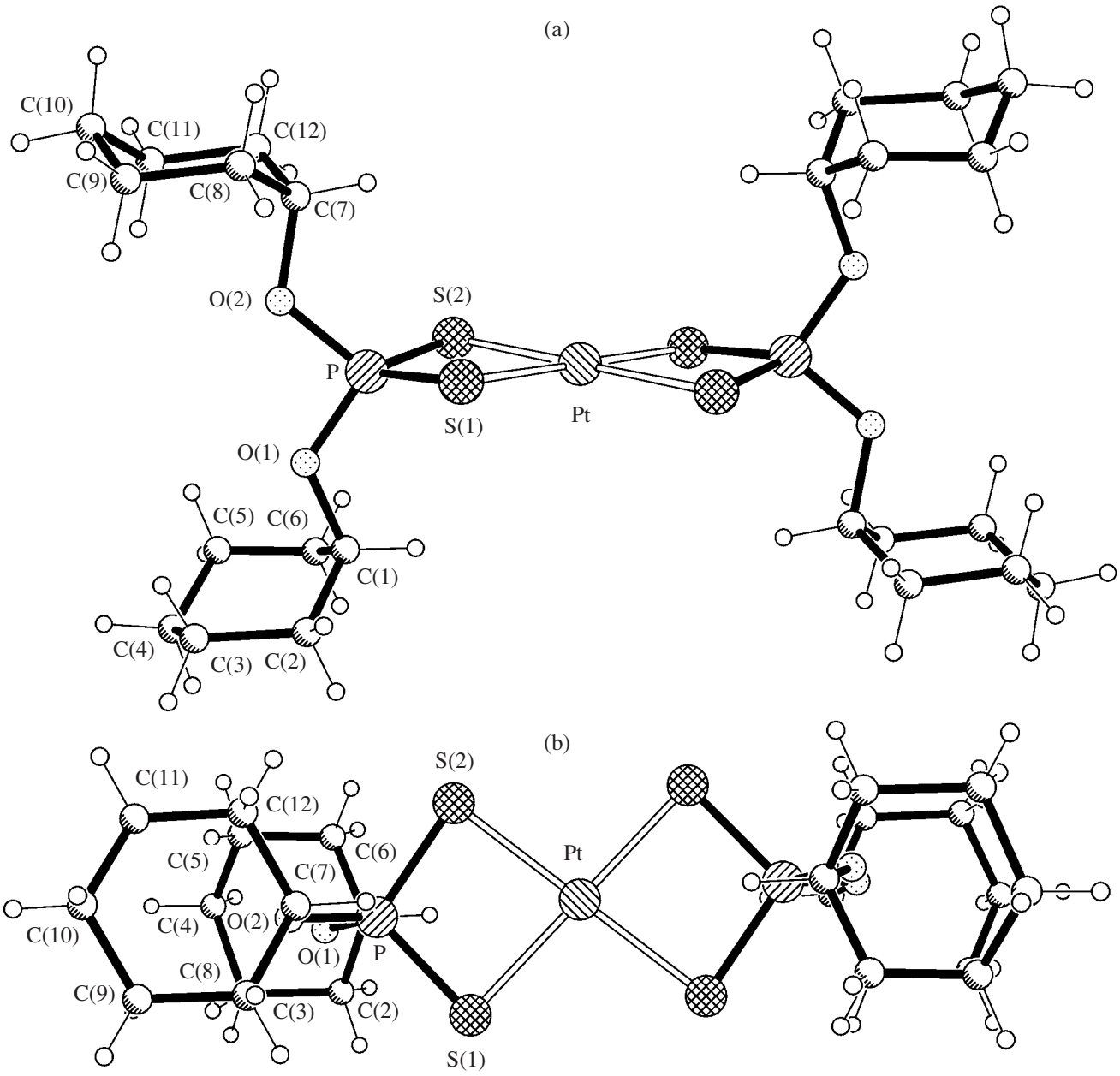

Fig. 7. Two projections of the molecular structure of $[Pt\{S_2P(O\text{-}cyclo\text{-}C_6H_{11})_2\}_2]$.

To sum up, we obtained crystalline platinum(II) and copper(II) complexes with O,O'-dicyclohexyl dithiophosphate and O,O'-diisopropyl dithiophosphate as ligands and characterized them by ^{13}C, ^{31}P, and ^{195}Pt CP/MAS NMR and EPR spectroscopy. The molecular structure of $[Pt\{S_2P(O\text{-}cyclo\text{-}C_6H_{11})_2\}_2]$ (**I**) results from S,S'-bidentate coordination of the Dtph ligands by platinum(II) to form the planar chromophore $[PtS_4]$ (X-ray diffraction data). For $[Pt\{S_2P(O\text{-}iso\text{-}C_3H_7)_2\}_2]$ (**II**), a new α-form was obtained and identified from ^{31}P MAS NMR spectra. For the platinum(II) complexes, we calculated the ^{31}P chemical shift anisotropy δ_{aniso} and the asymmetry parameter η.

ACKNOWLEDGMENTS

We are grateful to Cheminova Agro A/S (Denmark) for providing potassium O,O'-dialkyldithiophosphates.

This work was supported by the Russian Foundation for Basic Research and the Far East Division of the Russian Academy of Sciences (Program "Dal'nii Vostok", grant no. 06-03-96009).

REFERENCES

1. Gianini, M., Caseri, W.R., Gramlich, V., and Suter, U.W., *Inorg. Chim. Acta*, 2000, vol. 299, no. 2, p. 199.
2. Tkachev, V.V. and Atovmyan, L.O., *Koord. Khim.*, 1982, vol. 8, no. 2, p. 215.
3. Ivanov, A.V., Palazhchenko, V.I., Strikha, V.E., et al., *Dokl. Akad. Nauk* (Engl. Transl.), 2006, vol. 410, no. 4, p. 512.
4. Lawton, S.L., Rohrbaugh, W.J., and Kokotailo, G.T., *Inorg. Chem.,* 1972, vol. 11, no. 2, p. 612.
5. Pines, A., Gibby, M.G., and Waugh, J.S., *J. Chem. Phys.*, 1972, vol. 56, no. 4, p. 1776.
6. Earl, W.L. and van der Hart, D.L., *J. Magn. Reson.*, 1982, vol. 48, no. 1, p. 35.
7. Morcombe, C.R. and Zilm, K.W., *J. Magn. Reson.,* 2003, vol. 162, no. 2, p. 479.
8. Karaghiosoff, K., *Encyclopedia of Nuclear Magnetic Resonance*, Grant, D.M. and Harris, R.K.N.Y., Eds., New York: Wiley, 1996, vol. 6, p. 3612.
9. Kirakosyan, G.A., *Koord. Khim.,* 1993, vol. 19, no. 7, p. 507.
10. Press, W.H., Teukolsky, S.A., Vetterling, W.T., and Flannery, B.P., *Numerical Recipes in C*, Cambridge: Cambridge Univ., 1994.
11. Hodgkinson, P. and Emsley, L., *J. Chem. Phys.*, 1997, vol. 107, no. 13, p. 4808.
12. Antzutkin, O.N., Lee, Y.K., and Levitt, M.H., *J. Magn. Reson.*, 1998, vol. 135, no. 1, p. 144.
13. Wolfram, S., *The Mathematica Book,* Cambridge: Wolfram Media/Cambridge Univ., 1470.
14. *SMART and SAINT-Plus. Versions 5.0. Data Collection and Processing Software for the SMART System. Bruker AXS*, Inc. Madison (WI, USA), 1998.
15. *SHELXTL/PC. Versions 5.10. An Integrated System for Solving, Refining and Displaying Crystal Structures from Diffraction Data*, Bruker AXS Inc., Madison (WI, USA), 1998.
16. Ovchinnikov, I.V. and Konstantinov, V.N., *J. Magn. Reson.*, 1978, vol. 32, p. 179.
17. Rieger, Ph.H., *Electron Spin Resonance (Senior Reporter Symons M. C.R.)*, Newcastle upon Tyne: Athenaeum Press Ltd., 1993, vol. 13, p. 178.
18. Ivanov, A.V., Larsson, A.-C., Rodionova, N.A., et al., *Zh. Neorg. Khim.*, 2004, vol. 49, no. 3, p. 423 [*Russ. J. Inorg. Chem.* (Engl. Transl.), vol. 49, no. 3, p. 373].
19. Ivanov, A.V., Forsling, W., Kritikos, M., et al., *Dokl. Akad. Nauk*, 2000, vol. 375, nos. 1–3, p. 236.
20. Ivanov, A.V., Antzutkin, O.N., Forsling, W., et al., *Dokl. Akad. Nauk*, 2002, vol. 387, no. 4, p. 500 [*Dokl. Phys. Chem*. (Engl. Transl.), vol. 387, no. 4, p. 299].
21. Ivanov, A.V., Antzutkin, O.N., Larsson, A.-C., et al., *Inorg. Chim. Acta*, 2001, vol. 315, no. 1, p. 26.
22. Ivanov, A.V., Antzutkin, O.N., Forsling, W., and Rodionova, N.A., *Koord. Khim.*, 2003, vol. 29, no. 5, p. 323 [*Russ. J. Coord. Chem.* (Engl. Transl.), vol. 29, no. 5, p. 301].
23. Yin, Y.-G., Forsling, W., Bostrom, D., et al., *Chin. J. Chem*, 2003, vol. 21, no. 3, p. 291.
24. Ivanov, A.V., Gerasimenko, A.V., Antzutkin, O.N., and Forsling, W., *Inorg. Chim. Acta*, 2005, vol. 358, no. 9, p. 2585.
25. Larsson, A.-C., Ivanov, A.V., Antzutkin, O.N., et al., *Inorg. Chim. Acta,* 2004, vol. 357, no. 9, p. 2510.
26. Larsson, A.-C., Ivanov, A.V., Pike, K.J., et al., *J. Magn. Reson.*, 2005, vol. 177, no. 1, p. 56.
27. Larsson, A.-C., Antzutkin, O.N., Ivanov, A.V., and Forsling, W., *Centenary of Flotation Symposium*, Melbourne: (Brisbane, Queensland, Australia). The Australian Institute of Mining and Metallurgy, 2005, p. 497.
28. Ivanov, A.V., Zinkin, S.A., Gerasimenko, A.V., et al., *Koord. Khim.*, 2007, vol. 33, no. 1, p. 22 [*Russ. J. Coord. Chem.* (Engl. Transl.), vol. 33, no. 1, p. 20].
29. Ivanov, M.A., Antzutkin, O.N., Sharutin, V.V., et al., *Inorg. Chim. Acta*, 2007, vol. 360, no. 9, p. 2897.
30. Larsson, A.-C., Ivanov, A.V., Forsling, W., et al., *J. Am. Chem. Soc.*, 2005, vol. 127, no. 7, p. 2218.
31. Lawton, S.L. and Kokotailo, G.T., *Inorg. Chem.*, 1969, vol. 8, no. 11, p. 2410.